

LETTER TO THE EDITOR

## IV-VI resonant cavity enhanced photodetectors for the midinfrared

M. Böberl, T. Fromherz, T. Schwarzl, G. Springholz and W. Heiss †

Institut für Halbleiter- und Festkörperphysik, Universität Linz, Altenbergerstr. 69, 4040 Linz, Austria

**Abstract.** A resonant-cavity enhanced detector operating in the mid-infrared at a wavelength around  $3.6 \mu\text{m}$  is demonstrated. The device is based on a narrow-gap lead salt heterostructure epitaxially grown on a  $\text{BaF}_2(111)$  substrate. Below 140 K, the photovoltage clearly shows a single narrow cavity resonance, with a  $\Delta\lambda/\lambda$  ratio of only 2 % at 80 K.

arXiv:cond-mat/0409153v1 [cond-mat.mtrl-sci] 7 Sep 2004

† corresponding author: wolfgang.heiss@jku.at

## 1. Introduction

The sensitivity for detection of trace gas molecules in air or in other carrier gases by measuring the characteristic fingerprint like vibration-rotation absorption lines of molecules is in the spectral range of the mid-infrared by far higher than in the near infrared or in the visible. Thus, for sensitive gas analysis and atmospheric pollution monitoring highly efficient optoelectronic devices for the mid-infrared are required. Narrow-gap IV-VI semiconductors are promising candidates as mid-infrared detectors; polycrystalline IV-VI photodetectors operating at room temperature are even commercially available. In addition, two-dimensional PbTe focal plane arrays on a Si-substrate were realized recently [1]. For molecular spectroscopy, the emitter or detector or both have to be tuned to the molecule absorption line. This requisite can be achieved by either using a narrow band emitter and a broadband detector or a broadband source such as a glowbar and a detector with a small spectral bandwidth. In contrast to the above mentioned lead salt photodetectors, which have a relatively large spectral bandwidth, we demonstrate a photodetector with a small spectral bandwidth. In this so-called resonant cavity enhanced photodetector (RCEPD) a thin absorbing layer is placed in a vertical optical cavity. This yields advantages compared to conventional detectors because (a) the narrow detection wavelength of interest can be tuned by the cavity length and (b) the quantum efficiency is enhanced due to the standing wave effect caused by the cavity[2]. Up to now most work has been founded on RCEPDs operating in the near infrared for telecommunication purposes. These structures were fabricated from SiGe/Si layers [3] and from GaAs-based heterostructures [4, 5]. In the midinfrared first attempts on RCEPDs based on CdHgTe compounds [6] or fabricated of InAs [7] were demonstrated. These devices operate around  $3.1 \mu\text{m}$ .

In this work, we demonstrate a RCEPD based on the narrow gap lead salt semiconductors operating at a wavelength of  $\lambda = 3.6 \mu\text{m}$ .

## 2. Experiments

Figure 1 shows the schematic structure of the resonant cavity photodetector. The multilayer detector sample is grown by molecular beam epitaxy on (111)-orientated  $\text{BaF}_2$  that is transparent in the mid-infrared. The design of the lead salt RCEPD is similar to the design of IV-VI vertical-cavity surface-emitting laser structures [8, 9]. However, the RCEPD structure consists of only one Bragg mirror with a metallic mirror as second mirror. In detail, a two-period Bragg interference mirror consisting of  $\lambda/4$  thick  $\text{Pb}_{0.94}\text{Eu}_{0.06}\text{Te}/\text{EuTe}$  layer pairs acts as bottom mirror of the sample. The  $\text{Pb}_{0.94}\text{Eu}_{0.06}\text{Te}$  mirror layers are grown as digital alloy of PbTe and  $\text{Pb}_{0.59}\text{Eu}_{0.41}\text{Te}$  with a superlattice period of  $52 \text{ \AA}$ . Due to the high refractive index contrast of more than 80 % [10] between the two mirror materials, the two-period Bragg mirror exhibits a reflectivity as high as 98 %. The active region is composed of 3 PbTe/ $\text{Pb}_{0.95}\text{Eu}_{0.05}\text{Te}$  quantum wells (QWs) with a PbTe well width of  $50 \text{ \AA}$  and a  $\text{Pb}_{0.95}\text{Eu}_{0.05}\text{Te}$  barrier width of  $300 \text{ \AA}$ . On top of

the absorbing region, a 1.2  $\mu\text{m}$  thick  $\text{SiO}_2$  layer serving as insulator is deposited using plasma-enhanced chemical vapor deposition. The total length of the cavity complies with  $3\lambda/4$ , so that only one single resonance appears in the Bragg mirror stopband region. Mesas are fabricated using standard photolithography and wet chemical etching. On top of the mesas an Ag layer is sputtered serving as top cavity mirror. The active layer is contacted close to the top mirror mesa ensuring the optimal use of the resonant cavity effect. Gold wires are bonded on In pads forming a Schottky contact. For photoresponse experiments, the sample was mounted in a He flow cryostat. The samples were illuminated under normal incidence from the transparent substrate side using a glowbar. After passing a chopper and an optical low pass filter with a cut-off wavelength of 2.63  $\mu\text{m}$ , the radiation was focused on the sample. Photovoltage measurements were performed with a Fourier-transform infrared (FTIR) interferometer, which was operated in step-scan mode measuring the photovoltage by a standard lock-in technique. For all experiments, the device was operated under open-circuit conditions.

The structure was first characterized by FTIR reflectance experiments. The reflectivity spectrum of the sample measured at room temperature is shown as dashed line in Figure 2. It exhibits one clear cavity resonance of  $m=2^{\text{nd}}$  order due to the cavity length of three-quarter of  $\lambda$ . The resonance peak is at 3.45  $\mu\text{m}$  and has a full width at half maximum (FWHM) of about 70 nm which results in an effective finesse of 24. As shown in Figure 2, the width of the broad Bragg mirror stopband is more than 2  $\mu\text{m}$  owing to the high refractive index contrast of the mirror materials [10]. At the low-wavelength edge of the stopband (2.47  $\mu\text{m}$ ) an interference fringe from the total thickness of the structure appears. The two small dips in the reflectivity at 4.2  $\mu\text{m}$  are absorption lines from the remaining  $\text{CO}_2$  in the  $\text{N}_2$ -purged sample chamber.

In Figure 2, the photoresponse at 80 K of the device operating in photovoltaic mode is shown. The signal peak at 3.57  $\mu\text{m}$  corresponds to the position of the cavity resonance at 80 K. It is slightly shifted to higher wavelengths with respect to the cavity resonance observed in the reflectivity spectrum at room temperature due to the increase of the refractive index of the cavity materials with decreasing temperature. The linewidth of the cavity resonance in the photoresponse signal is only 80 nm corresponding to a small wavelength ratio  $\Delta\lambda/\lambda$  of 2 %. This linewidth is slightly larger than the width of the cavity resonance in the reflectance spectrum. This is due the fact that at 80 K, the active layer (the three thin PbTe QWs) acts as an absorber at the wavelength of the cavity resonance, while this is not the case at room temperature due to the strong temperature dependence of the PbTe bandgap. Therefore, at 80 K the cavity resonance is slightly damped and broadened leading to an increased linewidth in the photovoltage spectrum.

A small photovoltage signal is detected in the stopband region around the resonance (between the onset of the QW absorption at 4.5  $\mu\text{m}$  and 3  $\mu\text{m}$ ). This signal should be suppressed by the high reflectivity of the bottom Bragg mirror. However, because the

reflectivity of the Bragg mirror is only 98 % not all of the incoming light is reflected back. At smaller wavelengths than the stopband region ( $\lambda$  smaller than  $3.0 \mu\text{m}$ ) also a strong photovoltage signal is found. We assume that the  $\text{Pb}_{0.94}\text{Eu}_{0.06}\text{Te}$  layers of the Bragg mirror which absorb in this wavelength region contribute to the photovoltage signal. The cut-off of the photovoltage at  $2.63 \mu\text{m}$  is due to the used low-pass filter in the experimental setup.

Detector operation is observed up to 140 K. For the detector design we used in this work, the resonance in the photoresponse signal is quenched at 140 K, because the bandgap of the  $\text{PbTe}/\text{Pb}_{0.95}\text{Eu}_{0.05}\text{Te}$  QWs shifts to higher energies than the energy of the cavity resonance. This is due to the fact that the bandgap of the active material increases much stronger with increasing temperature than the refractive index decreases [11]. Designing the detector structure for a cavity resonance at higher energies, should allow obtaining detector operation temperatures reached by simple thermoelectric coolers.

### 3. Conclusions

We showed a lead salt resonant-cavity enhanced photodetector based on a two-period Bragg mirror and a metallic mirror and 3  $\text{PbTe}/\text{PbEuTe}$  QWs as absorbing material in between. The operation wavelength at 80 K is  $3.57 \mu\text{m}$  and the  $\Delta\lambda/\lambda$  ratio is only 2 %. By changing the cavity length, the resonance position can be tuned to a certain molecular absorption line, making such photodetectors a promising device for molecular gas sensing applications. This demonstration of the resonant-cavity-effect from a non-optimised structure gives prospect to gain suitable lead-salt photodetectors for gas absorption applications in the near future.

### Acknowledgments

The authors are grateful to S. Andreeva for technical assistance. Financial support from FWF (projects Y179 and P15583) and GME of Austria is gratefully acknowledged.

### References

- [1] Alchalabi K, Zimin D, Zogg H and Buttler W 2001 *IEEE Electron Device Letters* **22** 110
- [2] Ünlü M S, Kishino K, Chyi J-I, Arsenault L, Reed J and Noor Mohammad S 1990 *Appl. Phys. Lett.* **57** 750
- [3] Cheng Li, Huang C J, Buwen Cheng, Yuhua Zuo, Liping Luo, Jinzhong Yu and Qiming Wang 2002 *J. Appl. Phys.* **92** 1718
- [4] Heroux J B, Yang X and Wang W I 1999 *Appl. Phys. Lett.* **75** 2716
- [5] Kinsey G S, Gotthold D W, Holmes A L and Campbell J C 2000 *Appl. Phys. Lett.* **77** 1543
- [6] Pautrat J L, Hadji E, Bleuse J and Mangea N 1997 *J. Electronic Materials* **26** 667
- [7] Green A M, Gevaux D G, Roberts C, Stavrinou P N and Phillips C C 2003 *Semicond. Sci. Technol.* **18** 964
- [8] Fürst J, Pascher H, Schwarzl T, Böberl M, Heiss W, Springholz G and Bauer G 2002 *Appl. Phys. Lett.* **81** 208

- [9] Füst J, Pascher H, Schwarzl T, Böberl M, Springholz G, Bauer G and Heiss W 2004 *Appl. Phys. Lett.*
- [10] Heiss W, Schwarzl T, Roither J, Springholz G, Aigle M, Pascher H, Biermann K and Reimann K 2001 *Progress in Quantum Electronics* **25**, 193
- [11] Springholz G, Schwarzl T, Aigle M, Pascher H and Heiss W 2000 *Appl. Phys. Lett.* **76**, 1807

Figure captions

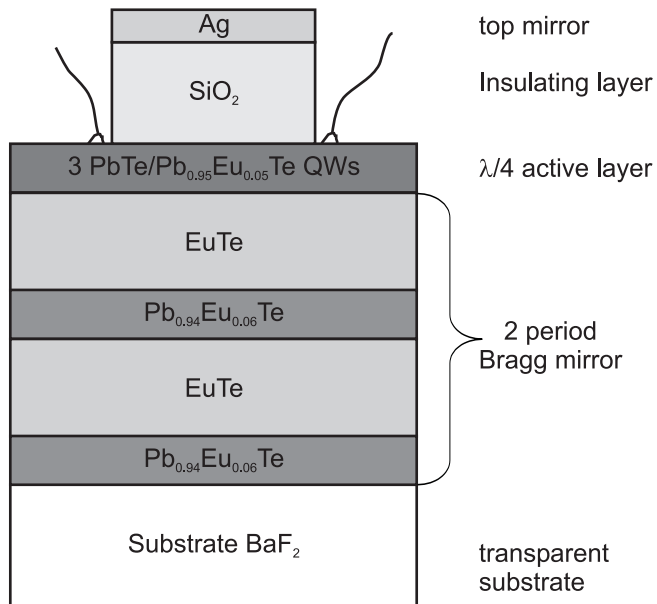
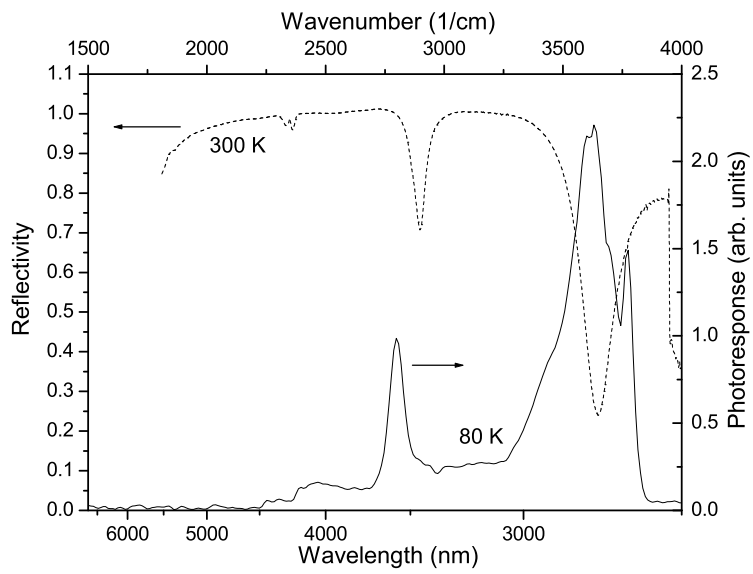


Figure 1. Schematic sketch of the resonant-cavity photodetector structure.



**Figure 2.** Room temperature reflectivity spectrum of the RCEPD structure (dashed line). Photovoltage of the structure measured at 80 K (solid line).